

Imaging surface/crystallographic shear plane intersections on the $\text{Mo}_{18}\text{O}_{52}(100)$ surface using scanning tunneling microscopy

Gregory S. Rohrer*, Weier Lu, Richard L. Smith and Anthony Hutchinson

Department of Materials Science and Engineering, Carnegie Mellon University, Pittsburgh, PA 15213, USA

Received 22 January 1993; accepted for publication 2 April 1993

The contrast in atomic-scale resolution scanning tunneling microscope (STM) images of the unreconstructed $\text{Mo}_{18}\text{O}_{52}(100)$ surface has been directly compared to components of the bulk structure. The features of interest that are identified in the STM images are the surface/crystallographic shear (CS) plane intersections and the different MoO_x coordination polyhedra. The intersection of the CS planes with the crystal surface creates a step-like feature that we call a “shear step” and MoO_4 groups have contrast that makes them appear larger or brighter than the MoO_6 groups. The identification of such features on this complex, yet well-ordered, surface will facilitate the interpretation of images from defective surfaces.

1. Introduction

The development of atomistic models to explain the chemical, electrical, and mechanical processes that occur at oxide surfaces relies on knowledge of the periodic and non-periodic (defects) components of the surface structure at the atomic level. Through the use of scanning tunneling microscopy (STM), this information is rapidly becoming available for compounds such as $\text{Bi}_2\text{Sr}_2\text{CaCu}_2\text{O}_{8+\delta}$ [1], TiO_2 [2], Fe_3O_4 [3], SrTiO_3 [4], $\text{Rb}_{0.33}\text{WO}_3$ [5]. One of the most exciting aspects of the results referred to above is that in most cases, surface inhomogeneities and defects were recorded in the STM images, features that are not easily detected using reciprocal space structure probes. Unfortunately, the interpretation of STM image contrast is not yet straightforward, especially from the components of the image that are not commensurate with the known bulk structure. The present difficulty in the interpretation of the contrast from defects limits the ultimate potential of this form of microscopy.

This difficulty was illustrated in a recent inves-

tigation of the reduced $\text{TiO}_{2-x}(110)$ surface in which unusual periodic features in atomic-scale STM images were explained by assuming that intergrowths of reduced Magnéli phases were present at the crystal surface [2]. These reduced phases differ from the bulk rutile structure only along widely separated crystallographic shear (CS) planes. Thus, the only new features of the surface structure are the surface/CS plane intersections. Similar CS plane structures have been used in the past to explain low energy electron diffraction patterns from WO_3 [6] surfaces and features in the photoelectron spectra of defective MoO_3 [7] and TiO_2 [8] surfaces. The intergrowth model has a number of merits which include concurrence of the experimental STM data with the expected periodicity and angular orientation of the surface features. However, the uncertain nature of the STM image contrast that would be expected at a surface/CS plane intersection adds ambiguity to the proposed explanation.

This particular ambiguity must be resolved if STM is to be used as a tool to study the surface defect structure of other materials such as the oxides of V, Nb, Mo, Ta, and W which also reduce via CS plane formation. We should men-

* To whom correspondence should be addressed.

tion that although the influence of CS planes on the properties of the oxide surface is not entirely clear, it stands to reason that the CS planes affect the lability of the material and ultimately the catalytic properties of these oxides. In fact, it has been suggested on the basis of both theoretical [9] and experimental work [10,11], that the surface/CS plane intersection is an active site for the partial oxidation of hydrocarbons. The potential importance of the relationship between the defect structure of these surfaces and their properties motivates us to unambiguously identify the STM image contrast associated with defects such as surface/CS plane intersections.

Thus, in order to clarify the effect that CS planes have on STM image contrast, we have examined (100) surfaces of single crystals of Mo₁₈O₅₂ using scanning tunneling microscopy. This compound has a known concentration and distribution of CS planes in the bulk which allows unambiguous assignment of the STM image contrast.

2. Experimental procedure

The single crystals used in this study were grown by chemical vapor transport following a method similar to that described by Bertrand et al. [12]. The procedure involves heating a sealed, evacuated silica ampoule containing a mixture of Mo, MoO₃, and I₂ in a horizontal tube furnace with a small temperature gradient. It is possible to obtain crystals under a number of different conditions, and some of the important parameters are described below.

The ampoules are approximately 10 cm long and have an inner diameter of 8 or 11 mm. Mo₁₈O₅₂ crystals were obtained from a variety of starting compositions. For example, while Mo–O starting compositions with the ideal O/Mo ratio of 2.89 yielded Mo₁₈O₅₂ crystals, large crystals were also obtained from charges with the hypostoichiometric ratio of 2.875. The ratio of the reactant mass to ampoule volume was varied from 0.06 to 0.2 g/cm³, with smaller ratios producing larger crystals. Repeated trials indicated that if other factors remained constant, increasing the

concentration of I₂ increased the size of the crystals; the highest concentration (mass I₂ to ampoule volume) used was 0.02 g/cm³. The reactants were heated for several days, maintaining a constant temperature at the hottest part of the furnace. Constant temperatures between 677 and 730°C gave similar results. We found that a 10°C temperature gradient across the length of the tube produced the largest crystals. Although a net transport of the reactants from one end of the tube to the other was not evident, isothermal experiments in a box furnace indicated that a measurable temperature gradient was needed to promote crystal growth.

The Mo₁₈O₅₂ crystals always appeared with other Mo–O phases. The phases were identified by separating large crystals into several groups based on color and morphology, grinding representatives of each group and recording powder diffraction patterns. Indexing the patterns and refining cell parameters demonstrated that each sample could be characterized as a single phase, the Mo₁₈O₅₂ phase being ubiquitous platey black crystals that were found in most growth trials. It should be pointed out that this phase is just one of a closely related family of shear compounds with the general formula Mo_nO_{3n-2}, and that the identification of the Mo₁₈O₅₂ crystals by the powder diffraction method does not rule out the likely possibility that the crystals contain up to 5 vol% of coherent intergrowths of related compounds such as Mo₁₉O₅₅ or Mo₂₀O₅₈ [13]. These related shear phases differ mainly in the spacing of the CS planes, which creates a unit cell of different dimensions.

The crystals cleave very easily perpendicular to the well-developed (100) faces due to the weak interlayer van der Waals bonding. Specimens were transferred to ultrahigh vacuum immediately following cleavage and imaged in the constant current mode ($I = 0.7$ nA) at -1.6 V sample bias (tunneling from filled states) using a clipped Pt–Ir tip. The images presented here that show atomic-scale features are representative of many observations, 42 of which were recorded. The features described in this paper were observed on several areas of three different specimens. From each image, a background plane has been sub-

tracted; this treatment eliminates the image tilt that would otherwise make atomic-scale features undetectable. No attempt has been made to correct the images for thermal drift, the primary source of image tilt and skew. The dimensions of surface periodicities were determined from two-dimensional Fourier transforms.

3. Results

Topographic images of the $\text{Mo}_{18}\text{O}_{52}(100)$ surface show that cleavage produces surfaces that are flat over hundreds to thousands of ångströms in each direction. There is, however, a characteristic periodic contrast which extends over all areas of the surface that were examined. The contrast (see fig. 1) has an average periodicity of 24 \AA and a topographic amplitude of approximately 2 \AA .

Higher resolution images reveal that this contrast is actually caused by a series of steps and terraces and that additional corrugations at smaller length scales exist within each terrace

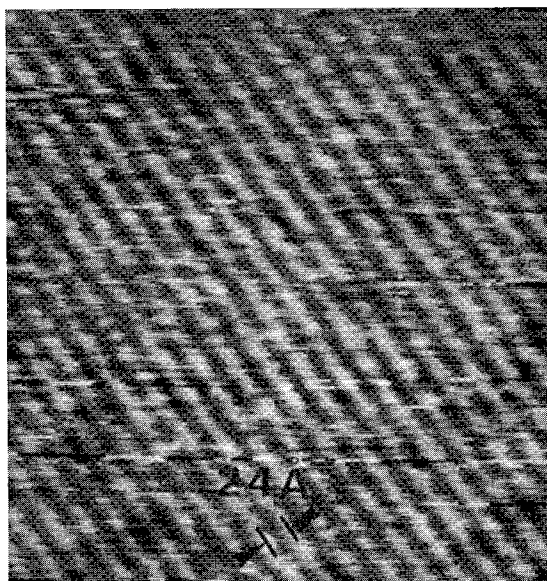


Fig. 1. Constant current STM image of a $440 \text{ \AA} \times 440 \text{ \AA}$ area of the surface. The unfiltered image is displayed with 4 \AA vertical resolution from black to white. The arrows mark the 24 \AA period of the corrugation.

(see fig. 2). Typically, the steps were very straight and evenly spaced, as shown in fig. 2a. Occasionally, however, curves and variations in terrace width are observed as can be seen in fig. 2b. At the edge of each step is a series of bright features which have an 11.8 \AA average frequency along the direction of the step. The topographic variation over these features is less than 1.0 \AA . There are also a series of rows within each step which have a periodicity of 3.8 \AA and a corrugation height of 0.4 \AA . Any additional features within these rows are incompletely resolved. The bright features at the step edge, with 11.8 \AA periodicity, occur at the end of every third row.

While the periodicity of features on images acquired from the same area within a short time period were consistent, there are noticeable variations between sets of data from different areas, acquired at different times. For example, if we describe the surface repeat unit as an oblique cell, the cell that best describes the structure in fig. 2a has the parameters $a = 26 \text{ \AA}$, $b = 11 \text{ \AA}$, and $\gamma = 98^\circ$, while the cell which best describes the structure of the surface in fig. 2b is $a = 23 \text{ \AA}$, $b = 13 \text{ \AA}$, and $\gamma = 103^\circ$. The variations in the two images presented here are characteristic of those observed among five different areas where high resolution images were recorded.

4. Discussion

The fact that $\text{Mo}_{18}\text{O}_{52}$ is a layered compound and cleaves along a van der Waals gap indicates that there should be no surface reconstruction and little relaxation, a condition that has been verified by reflection high energy electron diffraction studies [14]. The present paper exploits this situation to directly interpret the STM observations in terms of the bulk structure, the details of which have been specified by Kihlberg [15]. $\text{Mo}_{18}\text{O}_{52}$ is a triclinic structure with space group $\text{P}\bar{1}$ and two formula units per cell. This apparently complex structure is most easily understood as being derived from the simpler MoO_3 structure through a crystallographic shear operation. Stated briefly, if the perfect MoO_3 structure is first divided into 21 \AA thick slabs along $(35\bar{1})$

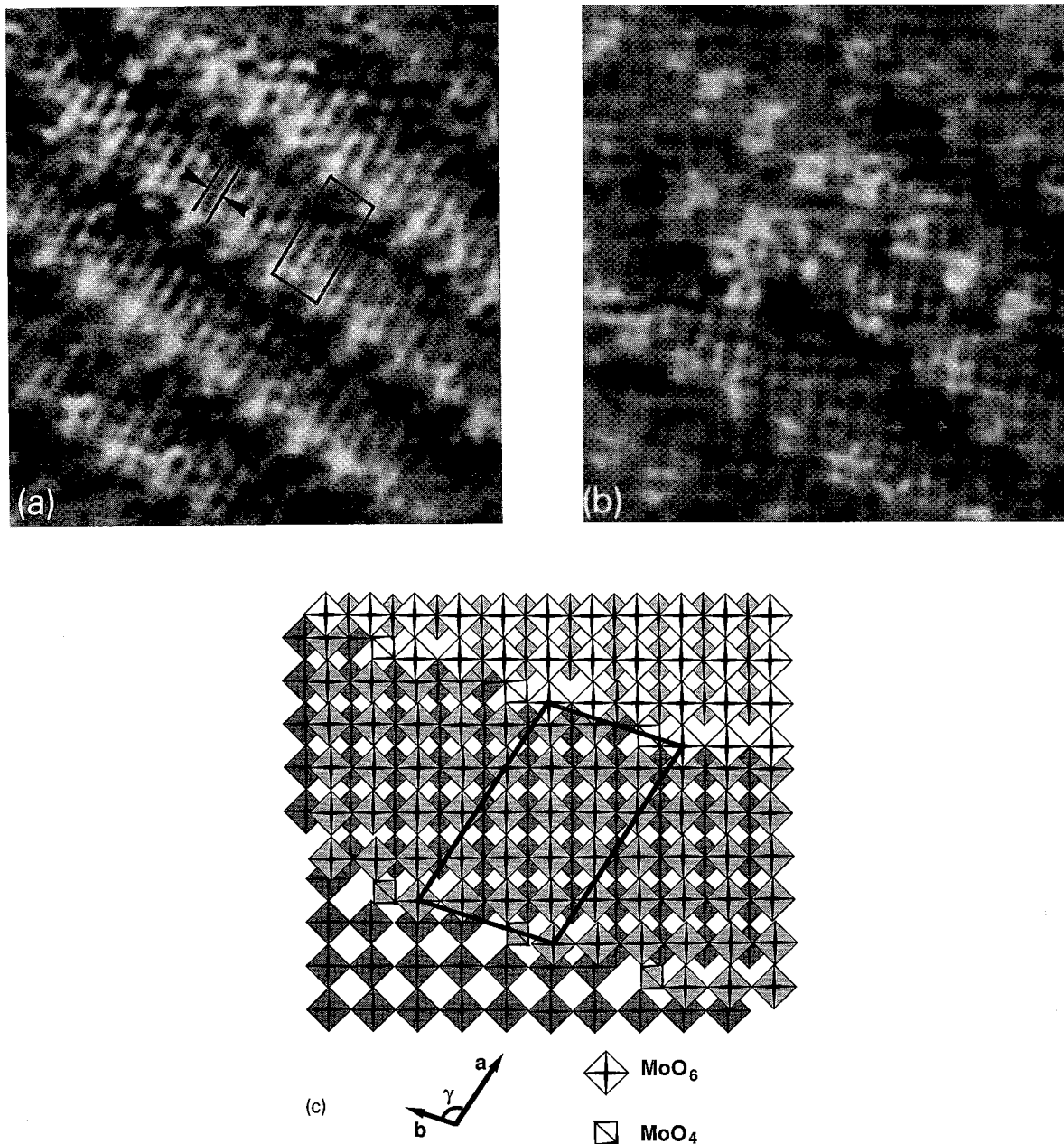


Fig. 2. (a) Constant current STM image of a $110 \text{ \AA} \times 110 \text{ \AA}$ area of the surface. The image is displayed with 2.5 \AA vertical resolution from black to white. The planar repeat unit is indicated by the bold lines, the 11.8 \AA periodicity by the shorter axis of this unit, and the 3.8 \AA periodicity of the rows of MoO_6 octahedra by the opposing arrows. (b) An image from a different area of the same crystal with the same dimensions and vertical resolution. Both of the images were filtered to remove high frequency noise. Fourier components with spatial wavelengths less than the smallest observed periodic surface corrugation were removed. (c) Polyhedral representation of a projection onto the (100) surface of $\text{Mo}_{18}\text{O}_{52}$. The polyhedra are shaded according to their vertical height, darker polyhedra are at lower levels. The shear steps are parallel to the b -axis and can be found where the contrast changes. Note the tetrahedral units at the edge of the shear step. The surface unit is indicated by the bold lines and the surface unit vectors are shown below.

planes, then the O atoms that lie on these boundary planes are eliminated, and finally each slab is moved relative to each other by the displacement $[\frac{1}{2}a - \frac{1}{6}b]$ and rejoined, the Mo₁₈O₅₂ structure is formed. Within each slab, the nearly ideal MoO₃ structure is retained, there is simply a modification of the coordination of some of the atoms at the shear plane boundary. The structural chemistry of the molybdenum oxides has been thoroughly described by Kihlberg [16] and details of the crystallographic shear process can be found in a review by Bursill and Hyde [17]. The critical aspect for this work is that the CS planes are ordered in such a way that there is one CS plane per unit cell and that the plane intersects (100) along the [010] direction every 21 Å.

The bulk unit cell parameters of Mo₁₈O₅₂ are $a = 8.145$ Å, $b = 11.89$ Å, $c = 21.23$ Å, $\alpha = 102.67^\circ$, and $\beta = 67.82^\circ$, and $\gamma = 109.97^\circ$ [15]. An STM image of the (100) surface is a two-dimensional projection onto the bc plane and, assuming no reconstruction, we expect the planar unit to be an oblique cell with $a = 21.23$ Å, $b = 11.89$ Å, and $\gamma = 102.67^\circ$. This cell, shown in fig. 2c, is in approximate agreement with the surface unit in the STM images and comparison with the structural model allows the assignment of topographic features. We should point out that while it is possible that the variations in the cell dimensions are caused by inhomogeneities in the sample due to intergrowths of other shear phases, we think it more likely that the differences are caused by varying degrees of thermal drift and that within this error, the observed unit cell sizes are consistent with one another and the expected cell. This conclusion is supported by two observations: that the spacings were always consistent within any given period of a few hours and that the surface cell parameter, b , which should be constant independent of the shear plane spacing, also varied among observations recorded at different times.

Based on their spacing and orientation with respect to other features, we conclude that the lines of contrast with the 24 Å periodicity are the surface/CS plane intersections. Using the bulk structure as a model, the vertical displacement between two terraces separated by a surface/CS plane intersection should be 1.7 Å. Measured

vertical displacements on the image vary from 1.5 to 2.5 Å, depending on the point of measurement. In order to differentiate these features from a normal step, formed at the termination of a surface plane, we call them "shear steps" and the area between "shear terraces". We believe that this is an important distinction because we wish to emphasize that this is an ideal (100) surface; the shear steps, which are part of the periodic structure, merely give it the characteristics of a vicinal surface.

The exact origin of the contrast within the shear terraces is difficult to specify without detailed knowledge of the electronic structure. Although such information is not available, we may reliably assume that during the formation of the images, electrons tunneled from occupied states in a partially filled π^* conduction band formed by the overlap of Mo 4d t_{2g}^3 and O 2p orbitals [18]. Because this band should be predominantly Mo 4d in character, we might assume that Mo atoms are preferentially imaged. However, the mixing of O 2p states in this band, taken together with the closer proximity of the apical oxygen atoms of the MoO₆ octahedra to the tip might lead one to conclude the O atoms are preferentially imaged. It is likely that both atom types make a contribution to the contrast and without attempting to deconvolute the competitive effects of orbital density and atomic proximity we will simply assume that it is the MoO_x group as a whole that is responsible for the contrast. This interpretation is consistent with explanations of the contrast in STM images of alkali molybdate bronzes, related compounds which can also be considered as arrangements of MoO_x polyhedra [19–22].

Based on this assumption, comparing the image to the polyhedral representation of the structure leads one to the conclusion that the observed corrugations are caused by the rows of corner sharing octahedra within each shear terrace. Perhaps the most interesting consequence of this conclusion is that it leads to an explanation for the bright spots that appear at the end of every third row at the edge of the shear step. The enhanced corrugation in the absence of any expected topographic rise suggests that the electronic density of states in this area is different. In

fact, the position and frequency of these spots correspond to the only positions on the surface where MoO₄ tetrahedral units occur. One possible reason for the pronounced contrast difference between the tetrahedral and octahedral units, based solely on geometric considerations, is that while a Mo atom in the octahedral environment is well shielded from the tip by the apical oxygen, in the tetrahedral unit there is a direct line between it and the tip which might lead to an enhanced local density of electronic states and the enhanced corrugations. Local differences in the electronic energy levels due to the different bonding configuration of the tetrahedral group and the connected octahedra probably also play a role. In any case, the two coordination polyhedra are clearly discriminated.

5. Conclusions

The (100) surface of Mo₁₈O₅₂ was imaged by STM and the observed features are interpreted by direct comparison with the bulk crystal structure. The intersection of CS planes with the surface creates small shear steps ordered in one dimension, giving the perfect (100) face of this crystal the characteristics of a vicinal surface. One surprising result is that constant current images discriminate between MoO₄ and MoO₆ groups, the tetrahedral groups appearing "larger" than the octahedral groups. Observations on this complex, yet highly ordered surface have allowed image contrast to be assigned to specific structural features which also occur on defective surfaces. It is our hope that such observations will pave the way for studies of randomly occurring defects on metal oxide surfaces.

Acknowledgements

This work was supported by the National Science Foundation under Grant DMR-9107305.

R.S. and A.H. thank the NSF Research Experience for Undergraduates program.

References

- [1] M.D. Kirk, J. Nogami, A.A. Baski, D.B. Mitzi, A. Kapitulnik, T.H. Geballe and C.F. Quate, *Science* 242 (1988) 1674.
- [2] G.S. Rohrer, V.E. Henrich and D.A. Bonnell, *Surf. Sci.* 278 (1992) 146.
- [3] R. Wiesendanger, I.V. Shvets, D. Bürgler, G. Tarrach, H.J. Güntherodt, J.M.D. Coey and S. Gräser, *Science* 255 (1992) 583.
- [4] T. Matsumoto, H. Tanaka, T. Kawai and S. Kawai, *Surf. Sci. Lett.* 278 (1992) L153.
- [5] W. Lu, N. Nevins, M. Norton and G.S. Rohrer, *Surf. Sci.*, to be published.
- [6] M.A. Langell and S.L. Bernasek, *J. Vac. Sci. Technol.* 17 (1980) 1296.
- [7] L.E. Firment and A. Ferretti, *Surf. Sci.* 129 (1983) 155.
- [8] V.E. Henrich, G. Dresselhaus and H.J. Zeiger, *Phys. Rev. Lett.* 36 (1976) 1335.
- [9] E. Brockawik and J. Haber, *J. Catal.* 72 (1981) 379.
- [10] S. Barber, J. Booth, R.D. Pyke, R. Reid and R.J.D. Tilley, *J. Catal.* 77 (1982) 80.
- [11] R.L. McCormick and G.L. Schrader, *J. Catal.* 113 (1988) 529.
- [12] O. Bertrand, N. Floquet and D. Jacquot, *J. Cryst. Growth* 96 (1989) 708.
- [13] L.A. Bursill, *Acta Cryst. A* 28 (1972) 187.
- [14] O. Bertrand, N. Floquet and D. Jacquot, *Surf. Sci.* 164 (1985) 305.
- [15] L. Kihlborg, *Ark. Kemi.* 21 (1963) 443.
- [16] L. Kihlborg, *Ark. Kemi.* 21 (1963) 471.
- [17] L.A. Bursill and B.G. Hyde, in: *Prog. Solid State Chemistry*, Vol. 7, Eds. H. Reiss and J.O. McCaldin (Pergamon, New York, 1972) p. 177.
- [18] M. Greenblatt, *Chem. Rev.* 88 (1988) 31.
- [19] J. Heil, J. Wesner, B. Lommel, W. Assmus and W. Grill, *J. Appl. Phys.* 65 (1989) 5220.
- [20] E. Garfunkel, G. Rudd, D. Novak, S. Wang, G. Ebert, M. Greenblatt, T. Gustafsson and S.H. Garofalini, *Science* 246 (1989) 99.
- [21] G. Rudd, D. Novak, D. Saulys, R.A. Bartynski, S.H. Garofalini, K.V. Ramanujachary, M. Greenblatt and E. Garfunkel, *J. Vac. Sci. Technol. B* 9 (1991) 909.
- [22] U. Walter, R.E. Thomson, B. Burk, M.F. Crommie, A. Zettl and J. Clarke, *Phys. Rev. B* 45 (1992) 11474.